Article

A Systematic Pipeline to Enhance the Fecal Metabolome Coverage by LC-HRMS

Marina A. Alves, [a,b] *Ana Carolina R. da Silva,* [a] *Clarisse L. Torres,* [a] *Lana R. de Almeida,* [c,d]
Ana Maria O. Mastella, [c] *Ricardo M. Borges* [e] *and Rafael Garrett* *,[a]

[a]*Laboratório de Metabolômica (LabMeta, LADETEC), Instituto de Química,
Universidade Federal do Rio de Janeiro (UFRJ), 21941-598 Rio de Janeiro-RJ, Brazil*

[b]*Turku Bioscience Centre, University of Turku and Åbo Akademi University, 20520, Turku, Finland*

[c]*Laboratório de Evolução, Sistemática e Ecologia de Aves e Mamíferos (BiMaLab),
Universidade Federal do Rio Grande do Sul, 91501-970 Porto Alegre-RS, Brazil*

[d]*Programa de Pós-Graduação em Biologia Animal, Universidade Federal do Rio Grande do Sul,
91540-000 Porto Alegre-RS, Brazil*

[e]*Instituto de Pesquisas de Produtos Naturais Walter Mors (IPPN),
Universidade Federal do Rio de Janeiro, 21941-599 Rio de Janeiro-RJ, Brazil*

The comprehended knowledge of the metabolic profile of the fecal matter has been recognized as an important point for understanding metabolic changes in the human systemic metabolism and it can provide precious information about host-gut microbiota interactions. However, few analytical strategies have been addressed for a broad analysis of metabolites with different chemical properties to better understand the chemical space of fecal samples. Here we report a systematic pipeline to achieve comprehensive coverage of the fecal metabolome, from high polar to nonpolar metabolites, using dog fecal samples as a proof-of-concept. This pipeline comprises a monophasic (ACN/H$_2$O) and a biphasic extraction (methyl *tert*-butyl ether (MTBE)/MeOH/H$_2$O) of the sample, followed by three liquid chromatography-high resolution tandem mass spectrometry (LC-HRMS/MS) methods using HILIC-amide, RP-C$_{18}$ and CSH-C$_{18}$ columns, and a switch polarity acquisition mode in the electrospray ion source. This approach allowed the annotation of 376 metabolites from 70 different chemical classes. The chemical space analysis by molecular networking and the pathway analysis revealed the complexity of the fecal sample and the importance of combined methods to better understand biochemical pathways. This pipeline can be used as a valuable tool to comprehend the relationship between host-gut microbiota metabolites and the influence of diet, medication, or environmental changes.

Keywords: LC-HRMS, metabolomics, lipidomics, fecal, molecular networking

Introduction

During the last years, the fecal analysis by mass spectrometry has emerged as an important field to provide insights into the relationship between the host and the gut microbiome activity and how it can affect the host homeostasis.[1-3] This symbiotic relationship has been shown to play a vital function in human metabolism, immunity, and reaction to diseases, such as diabetes,[4,5] coronary artery disease,[6] inflammatory disorders,[7] but also for the organism health state.

The metabolites produced by the gut microbiome, and other compounds that comprise the fecal matter, greatly varies and can be modified according to changes in host metabolism, such as age,[8] species,[9] diet,[10] disease,[3] or therapeutic intervention.[11] In this way, the fecal matter that has been classically used for microbiological analyses has gained other applications with the advance of the knowledge of endogenous and microbial metabolites using omics approaches.

Mass spectrometry (MS)-based metabolomics and lipidomics have been revealed as important tools to study fecal samples. This is mostly due to the high sensitivity, specificity, and broad coverage of different classes of compounds by the mass spectrometer, especially when

*e-mail: rafael_garrett@iq.ufrj.br

coupled to separation techniques, such as liquid or gas chromatography.[1,2,12-16]

The use of animal fecal samples as a model for method development has been reported by several authors.[17-21] For instance, pig fecal samples were analyzed by gas chromatography-mass spectrometry (GC-MS) and liquid chromatography-mass spectrometry (LC-MS), and around 300 compounds were identified.[18] Another study described the use of bovine feces to develop an liquid chromatography-high resolution mass spectrometry (LC-HRMS) based metabolomic approach to generate an informative fingerprint of this sample.[17] To evaluate the pig fecal metabolome change after grape seeds consumption by the animals, LC-HRMS metabolomics and lipidomics were applied and revealed that cholesterol, bile acids, and purine metabolites were some of the compounds altered due to the seed consumption.[22] However, a methodology that combines both polar and nonpolar metabolite analyses, covering the fecal metabolome and lipidome via LC-MS can be a prospective strategy and has not been thoroughly evaluated.[3,23,24] Thus, this study aimed to implement a pipeline for a comprehensive metabolite profile of fecal samples. Therefore, a combination of extraction methods using a monophasic and a biphasic system and LC separation using three columns with distinct separation mechanism were tested to extract and analyze from high polar compounds (e.g., sugars, organic acids and amino acids) to weakly polar and nonpolar compounds (e.g., lipids) in dog fecal samples. Moreover, a molecular networking analysis was used to evaluate the results from the LC-HRMS/MS data to reveal the complexity of the chemical space of the fecal samples and the pathway analysis was shown to benefit from that broader coverage of the fecal samples.

Experimental

Chemicals

The methyl *tert*-butyl ether (MTBE), acetonitrile (ACN), and methanol (MeOH) were high performance liquid chromatography (HPLC) gradient grade and obtained from Tedia (Fairfield, OH, USA). Ammonium formate and formic acid were purchased from Merck (São Paulo, Brazil). High-purity water (18.2 MΩ cm) was prepared using a Millipore Milli-Q (Billerica, MA, USA) purification system.

Fecal material

A triplicate of fecal samples deposited in the environment from three domestic dogs (*Canis lupus familiaris*) were collected by their owners in 50 mL Falcon tubes during three different days (9 samples in total) and sent to the

laboratory for processing. This step included drying the fecal samples for 4 h in an oven at 60 ºC followed by a 1 h rest in a fume hood. Then, samples were weighted to the nearest 0.1 mg. This process was repeated until the samples reached a constant mass (4-5 cycles).[25] Afterward, the samples were ground with a mortar and pestle and standardized to a sieve size of 180 mm. In contrast to fresh, fresh-frozen, or freeze-dried fecal samples generally used in metabolomic studies,[1] the oven-dry method was employed for this dog fecal samples since this study is part of a larger project about analyses of dried animal feces deposited in the environment. Animal handling and fecal analysis were in accordance with the ethical standards and registered at Federal University of Rio Grande do Sul (Research and Ethics Committee License 28645).

Sample extraction

A pool of dried fecal samples (n = 9) was used to perform two extraction protocols: (*i*) protocol A, for the extraction and separation of lipids from polar metabolites, and (*ii*) protocol B, for the non-selective extraction of metabolites.

(*i*) Protocol A: the lipid and polar compounds extraction were performed according to the Matyash *et al.*[26] protocol. Methanol (300 μL) was added to 100 mg of the powder dog feces pool (n = 3) in a microtube of 2.0 mL and vortexed at 3000 × g for 30 s. Then, 1.0 mL of MTBE was added, and the mixture was submitted to an ultrasonic bath for 15 min, followed by the addition of 250 μL of water. After 10 min at 4 ºC, the sample was centrifuged at 9000 × g for 15 min. The organic (upper) phase was transferred to a new microtube, and the aqueous phase was re-extracted with 400 μL of 10:3:2.5 (v/v/v) MTBE/MeOH/H_2O. Both phases were dried under nitrogen flow at 40 ºC and stored at −20 °C until analysis.

(*ii*) Protocol B: the non-selective extraction, adapted from Zeng *et al.*[16] and Zalloua *et al.*[27] was performed extracting the fecal sample pool (n = 3) at a ratio of 1:10 (m/v) with 1.0 mL of ACN:H_2O (1:1, v:v), vortexed at 3000 × g for 30 s, sonicated for 15 min at room temperature, and vortexed again. After centrifugation at 9000 × g for 15 min, 400 μL of the supernatant was transferred to a microtube and stored at −20 °C until analysis.

LC-HRMS/MS analyses

Samples were analyzed by a DionexUltiMate 3000 liquid chromatography coupled to a hybrid Quadrupole-Orbitrap high-resolution mass spectrometer (Thermo Scientific, Frenton, CA, USA) equipped with an electrospray

ionization (ESI) source and externally calibrated using the ready-to-use Thermo Pierce (Waltham, MA, United States) ESI positive or negative ion calibration solutions.

For the LC-HRMS/MS analysis of lipids from protocol A, samples from the dried organic phase were reconstituted in 50 µL of isopropanol:ACN:H$_2$O (2:1:1; v/v). Chromatographic separation was performed in a Waters XSelect CSH C$_{18}$ column (150 × 2.1 mm; 2.5 µm particle size) in gradient elution mode using ACN:H$_2$O (60:40, v/v) as mobile phase A and isopropanol:ACN (90:10, v/v) as mobile phase B, both with 0.1% formic acid and 10 mM ammonium formate. The gradient elution was as follows: 0-2.0 min 40% B; 2.0-2.1 min 43% B; 2.1-12.0 min 50% B; 12.0-12.1 min 54% B; 12.1-18.0 min 70% B; 18.0-18.1 min 99% B; 18.1-25.0 min 40% B.[27] The column temperature was set to 45 °C and the solvent flow rate was 0.4 mL min^{-1}. The injection volume was 6 µL and samples were analyzed by polarity switching between the positive and negative ESI modes. Mass spectrometry conditions were: spray voltage 3.9 kV for ESI+ or −3.6 kV for ESI−, ion transfer capillary temperature 320 °C, sheath and auxiliary gases 45 and 20 arbitrary units, respectively, normalized collision energy (NCE) of 20 for ESI+ and 25 for ESI−. Data were acquired in full scan over *m/z* range of 120-1000 Da at a resolution of 35.000 (full width at half maximum (FWHM)) followed by ddMS2 Top 3 experiment at a resolution of 17,500.[27,28]

For the LC-HRMS/MS analysis of polar metabolites from protocol A, samples from the dried aqueous phase were reconstituted in 50 µL of ACN:H$_2$O (1:1; v/v). For the chromatographic separation, a Waters Xbridge Amide column (150 × 4.6 mm; 3.5 µm particle size) was used and maintained at 40 °C. The separation was performed in gradient elution mode at a flow rate of 0.5 mL min^{-1} using H$_2$O containing 10 mM ammonium acetate and 0.04% ammonium hydroxide as mobile phase A, and ACN:H$_2$O (95:05, v/v) containing 10 mM ammonium acetate and 0.04% ammonium hydroxide as mobile phase B. The injection volume was 4 µL. The gradient used was as follows: 0-2 min 95% B; 2-18 min 50% B; 18-21 min 50% B; 21-22 min 95% B; 22-28 min 95% B.[29,30] Samples were analyzed by polarity switching between the positive and negative ESI modes. Mass spectrometry conditions were: spray voltage of 3.9 kV for ESI+ and 3.6 kV for ESI−, ion transfer capillary temperature 300 °C, sheath gas flow and auxiliary gas 50 and 10 arbitrary units, respectively, 15-40 eV NCE. Data were acquired in full scan experiments over a *m/z* range of 100-1000 Da at a resolution of 35,000 (FWHM) followed by ddMS2 Top 3 experiment at a resolution of 17,500 resolution.

For the LC-HRMS/MS analysis of metabolites from protocol B, the chromatographic separation was performed

in a Thermo Syncronis RP C$_{18}$ column (50 × 2.1 mm; 1.7 µm particle size) maintained at 40 °C in gradient elution mode at 350 µL min^{-1} using 0.1% formic acid in H$_2$O:ACN (95:5, v/v) as mobile phase A and 0.1% formic acid in H$_2$O:ACN (5:95, v/v) as mobile phase B. Gradient elution was performed as follows: 0-0.5 min 5% B; 0.5-4 min 60% B; 4-9 min, 100% B; 9-12 min 100% B; 12-12.1 min 5% B; 12.-16 min 5% B. Sample injection volume was 4 µL. Samples were analyzed by polarity switching between the positive and negative ESI modes. Mass spectrometry conditions were: spray voltage 3.6 kV for ESI+ and 3.1 kV for ESI−; capillary temperature 320 °C; sheath and auxiliary gases 45 and 15 (arbitrary units), respectively, 15-35 NCE. Samples were analyzed in the scan range of *m/z* 120 to 1000 Da at a resolution of 35,000 (FWHM) followed by ddMS2 Top3 experiments using a resolution of 17,500.[31]

Data processing, compound annotation, and classification

LC-HRMS/MS data were analyzed by the Thermo Xcalibur software v3.0 and processed by a lipidomics and metabolomics workflow using the MS-Dial software (RIKEN, version 4.24).[32] This workflow included peak detection, deconvolution, alignment, background subtraction, and compound annotation using a default MS/MS library for lipid analysis and a customized MS/MS database that included the MassBank of North America and NIST 2014 MS/MS libraries for polar and weakly polar metabolites (parameters described in Tables S1-S3, Supplementary Information (SI) section). An error between the experimental *vs.* theoretical formula ≤ 5 ppm (but ≤ 8 ppm for *m/z* values below 250 in ESI−) and a similarity score of MS/MS spectra higher than 80% were considered. This higher mass accuracy error used for *m/z* values below 250 in ESI− was due to the mass range (265-1680 Da) of the external calibration solution employed in this study. Aiming to prevent false positive/ negative peak identification, data were manually inspected to verify spectral matches with the database.

The resulting annotated compound list was classified according to the Chemical Classification Dictionary using the chemical hierarchy classification system ClassyFire.[33] This web platform allowed subclass chemical levels from known chemical compounds. ClassyFire requires Simplified Molecular-Input Line-Entry System (SMILES) as input, which was obtained using the web-based Chemical Translation Service.[34] Venn diagrams were created using the Bioinformatics and Evolutionary Genomics website tool.[35]

The pathway analysis was performed using the HMDB (Human Metabolome Database) IDs of the

annotated metabolites from the multiple LC-HRMS analytical conditions by Pathway Analysis module of the MetaboAnalyst 4.0 web application.[36] After uploading the data, these annotated compounds were subsequently compared with those compounds contained in the pathway library. There are three outcomes from the step: exact match, approximate match (for common names only), and no match. Compounds without a match were excluded from the subsequent pathway analysis. The pathway step was performed by selecting the Kyoto Encyclopedia of Genes and Genomes (KEGG) database and HMDB libraries. The pathway topology analysis used betweenness centrality measure to estimate node importance. Therefore, the total/maximum importance of each pathway is 1. The impact pathway score and statistical *p* values were used as a measure to identify the altered metabolic pathways. The pathway impact score was calculated based on the number of matched metabolites from datasets to a particular metabolic pathway (threshold was set to > 0.1) and *p*-value ≤ 0.05 was considered as significant.

Molecular networking

The LC-HRMS/MS datasets collected from the three different columns were pre-processed separately using the MS-Dial software[32] to generate three MGF files containing the MS/MS information from each aligned dataset. These MGF files were submitted to Molecular Networking using the Classical workflow[37] as separate groups, but with the MS-Cluster option disabled so that each cluster represents a feature across the different datasets.[38] This is the basis of what became a role separate workflow, the Feature-Based Molecular Networking.[39,40] The precursor ion mass tolerance was set to 0.02 Da and the MS/MS fragment ion tolerance 0.02 Da. The networks were created where edges were filtered to have a cosine score above 0.8 and more than 4 matched peaks. In this setup, data from the RP-C_{18}, the CSH-C_{18} and the HILIC-amide columns were analyzed as independent samples. Following a routine pipeline for chemical family classification, the workflows MS2LDA (including the MotifDB created from GNPS, MassBank and Urine available from the GNPS platform) and MolNetEnhancer were applied.[41,42] The resulting networks were plotted using the Cytoscape software.[43]

Results and Discussion

Set up of the extraction method

This study aimed to implement a comprehensive pipeline for the analysis of nonpolar and weakly polar metabolites (e.g., lipids, bile acids, etc.) to high polar metabolites (e.g., sugars, organic acids, amino acids, etc.) in fecal samples by untargeted metabolomic and lipidomic approaches. Thus, to expand the metabolite coverage, we recognized the limitation involved in the use of a single extraction procedure, due to the limited selectivity of the extractor solvent. As well as the use of a single LC column due to the preferential types of chemical interactions between the stationary/mobile phases and the metabolites, such as the hydrophobic interactions for C_{18} columns and the hydrophilic interactions for HILIC columns since it may hamper the proper analysis different classes of compounds.

To investigate the sample extraction scale that could provide efficient recovery of different classes of metabolites, a preliminary test was performed using 20 and 100 mg of dried fecal samples extracted by 200 and 1000 μL of $ACN:H_2O$ (1:10 m/v ratio, protocol B), respectively. Figure 1 shows the LC-HRMS base peak chromatograms for a fecal sample extracted by 100 mg *per* 1000 μL (Figure 1A) *vs.* 20 mg *per* 200 μL (Figure 1B). Despite having the same sample-to-solvent ratio, a clear difference was observed between the two chromatograms, with the 100 mg *per* 1000 μL scale showing a higher number of LC peaks and signal intensity. Besides, this scale allowed more MS acquisition points *per* peak, as well as a higher number of MS/MS spectra acquired because of the higher abundance of the peaks. To exemplify, an extracted ion chromatogram for the *m/z* 300.29007 [M + H]⁺ (a, Figure 1C) is shown in b (Figure 1C), where it is possible to observe more than 10 data points acquired and its MS/MS spectrum (c, Figure 1C) of high intensity and low background signals. This difference in LC-HRMS chromatogram quality by methods of different scale could be due to a difficulty in sample homogenization in the microtube by the 20 mg *per* 200 μL proportion, especially because the solution obtained presented a high number of particulates before centrifugation, reducing the contact area between the sample and the solvent, leading to an inefficient extraction compared to the larger scale procedure.

LC-HRMS/MS analysis and metabolite annotation

The information from the preliminary test was used to establish the pilot project (Figure 2) for a comprehensive fecal analysis. In protocol A (Figure 2) MTBE/MeOH/H_2O was used as extraction solvent aiming to retain more hydrophobic species in the upper organic phase, beneficial for the lipid extraction.[26] Simultaneously, the polar metabolites were extracted in the lower aqueous fraction. The LC-HRMS/MS analyses of the extracts from protocol A were performed using the HILIC-amide column
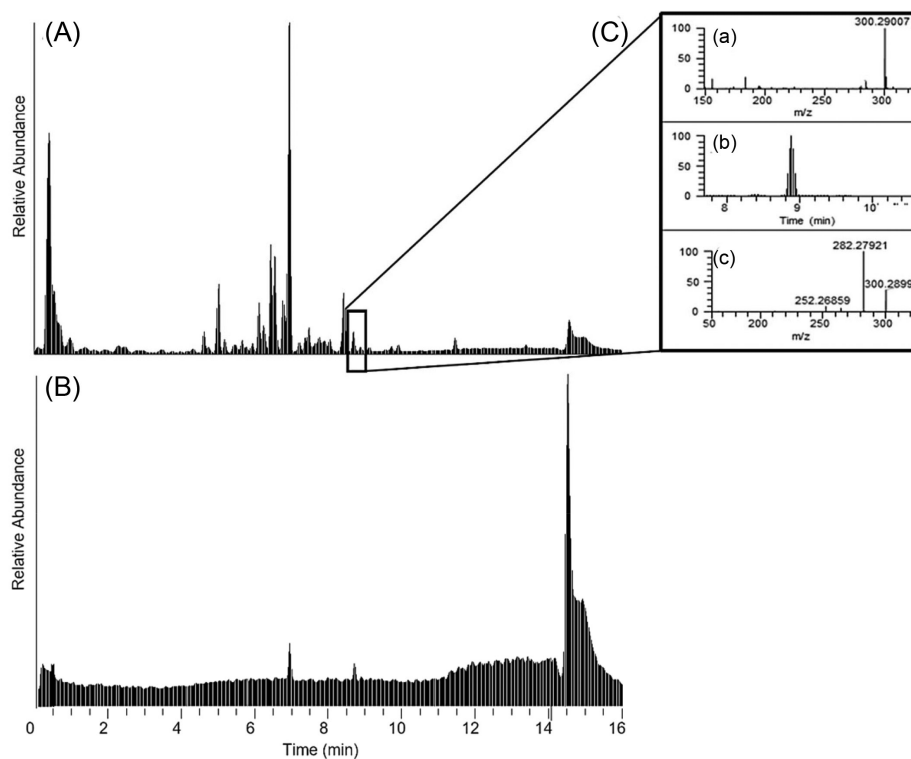
Figure 1. LC-ESI(+)-HRMS base peak chromatograms in a RP-C$_{18}$ column demonstrating a preliminary scale study using in (A) 20 mg and (B) 100 mg of dried fecal samples extracted by ACN:H$_2$O (1:1 v/v). The insert (C) shows the precursor ion of *m/z* 300.29007 [M + H]$^+$ (a), which generated a chromatographic peak at 8.8 min with high acquisition points (b) and the MS/MS spectrum in (c).

for the polar aqueous fraction, while the CSH-C$_{18}$ column was used for the lipid fraction. In parallel, the protocol B was performed using the same amount of fecal sample (100 mg) but using ACN/H$_2$O as the extraction solvent and injection in a RP-C$_{18}$ column to cover a broad range of metabolites. Thereby, three chromatographic conditions were employed to delineate a full view of metabolites in the fecal sample.

Typical LC-HRMS base peak chromatograms of a dog fecal sample and the elution order of some representative classes of compounds according to the ClassyFire subclass classification are shown in Figure 3. To analyze the metabolites detected exclusively and not exclusively in each ESI mode and chromatographic column, the raw data generated from all samples were submitted to the metabolomic and lipidomic workflows of MSDial 4.24 software.[32] Compounds were putatively identified according to the Metabolomics Standards Initiative as level 2.[44,45]

A total of 77 metabolites were annotated from the HILIC-amide analysis. Among these, 49 compounds were detected in the positive ion mode (ESI+) and 30 compounds were detected in the negative (ESI−) (2 compounds, hypoxanthine and *N*-acetylmuramic acid, were detected in both polarities) (Table S4, SI section). The RP-C$_{18}$ chromatographic method contributed with 96 annotated compounds in the ESI+ and 64 in ESI− (160

in total) (Table S5, SI section,), while the analysis using the CSH-C$_{18}$ column resulted in 152 annotated compounds (90 and 70 metabolites for ESI+ and ESI−, respectively, and 17 in common for both polarities) (Table S6, SI section). The diverse number of annotated compounds in both polarities demonstrated the importance of the fast polarity switching for complementary metabolite annotation and construction of the metabolic space under study. Furthermore, it allowed the collection of a vast amount of data in just one sample injection, reducing the number of injected samples since the pipeline proposed here relies on the analysis of the same fecal sample in three LC columns. Recently, Villaret-Cazadamont *et al.*[46] also proposed an optimized approach with a biphasic acidified extraction method (ACN/MeOH/H$_2$O) to perform LC-MS metabolomics and lipidomics analyses. Schwaiger *et al.*[47] analyzed plasma samples combining metabolites and lipids extracts using a HILIC and RP-C$_{18}$ performed in parallel. However, there are still few examples of this integrated strategy to cover an extensive vision of metabolites using fecal matter.

We conducted a study to measure the chemical relevance of the annotated compounds. For this purpose, the distribution of identified compounds belonging to chemical classification families was performed according to the web-based application ClassyFire.[33] This platform
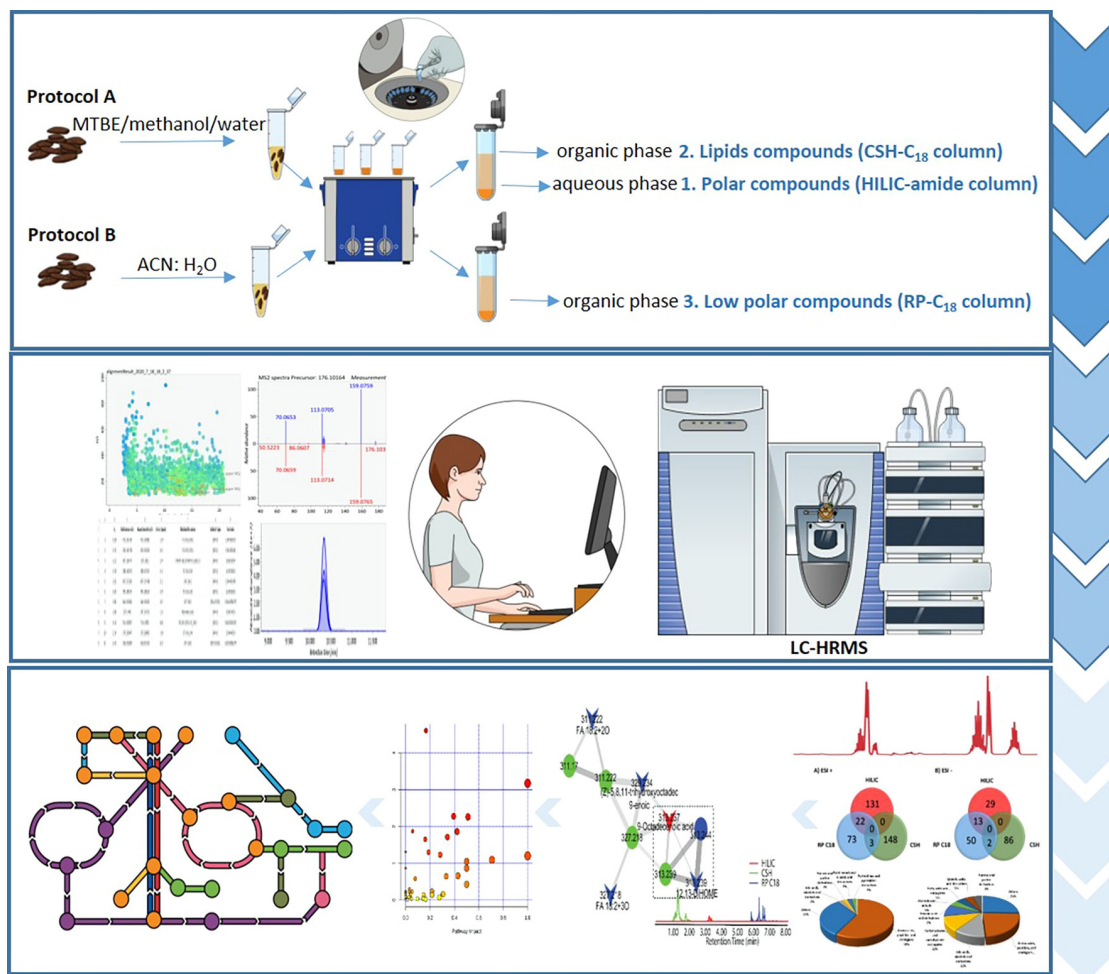
Figure 2. Schematic pipeline applied for the comprehensive analysis of fecal samples by LC-HRMS.
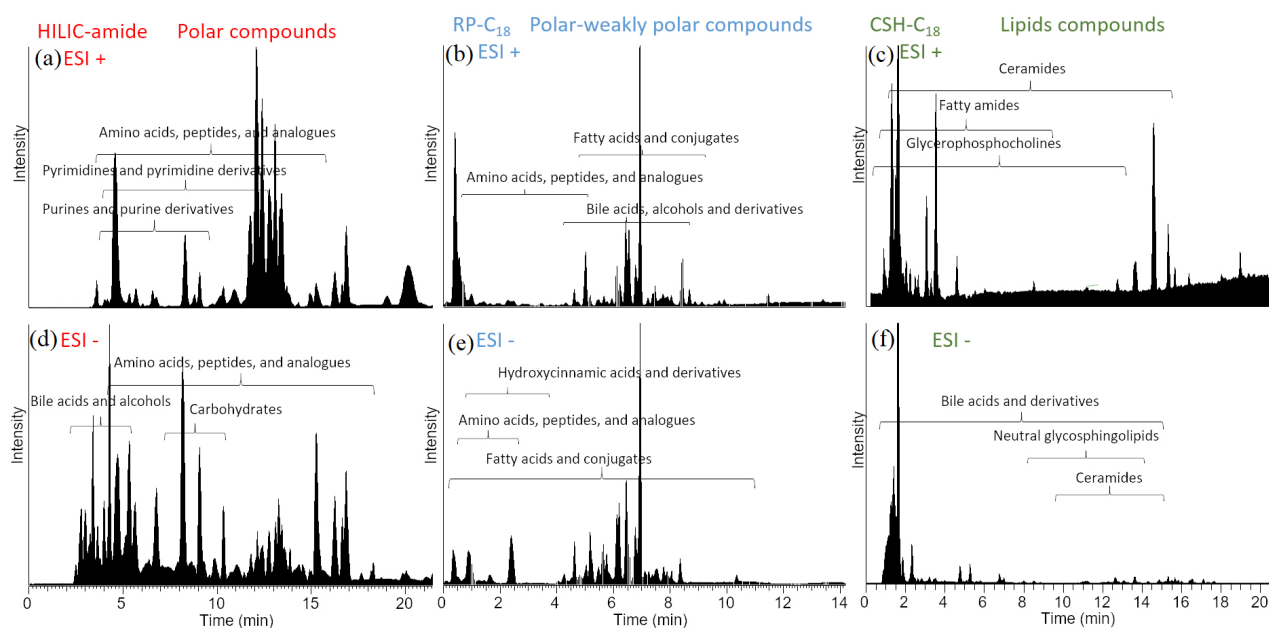

Figure 3. LC-HRMS base peak chromatograms of fecal samples from the three chromatographic conditions in positive and negative-ESI modes. Representative classes of compounds according to the ClassyFire subclass classification are shown in the figures. (a), (b) and (c) show the separation performed in positive mode using the HILIC-amide, RP-C$_{18}$ and CSH-C$_{18}$, respectively; (d), (e) and (f) show the separation performed in negative mode using the HILIC-amide, RP-C$_{18}$ and CSH-C$_{18}$, respectively.

allows chemical classification and description from known chemical compounds up to 11 different levels (Kingdom, SuperClass, Class, SubClass, etc.). Based on the common characteristic and structural properties of the compounds, the annotated metabolites from the different chromatographic columns were classified within categories and levels. The ClassyFire subclass was chosen to classify the compounds annotated in this study. The HILIC-amide classification in ESI+ and ESI− are exemplified in Figure 4. As it can be seen (Figure 4a), of a total of 23 ontologies classes, amino acids, peptides, and analogs; bile acids, alcohols and derivatives; purines and purine derivatives; and fatty acids and conjugates; were the classes with a higher number of identified compounds, presenting 21, 3, 3 and 2 metabolites, respectively, in the ESI+. In the ESI− (Figure 4b) a total of 16 classes were found, including amino acids, peptides, and analogues; benzoic acids and derivatives; carbohydrates and carbohydrate conjugates; and bile acids, alcohols and derivatives; as wide subclasses of annotated metabolites: 4, 4, 4, 3 compounds, respectively. Thereby, the amino acids, peptides, and analogs family exhibited the highest distribution in both ESI modes. In contrast, the chemical profile of the metabolic families had different classifications between ESI+ and ESI−.

Compounds annotated by the RP-C$_{18}$ column were classified into 28 subclasses in the ESI+ and 21 in the ESI−. The subclasses fatty acids and conjugates; amino acids, peptides, and analogs; and flavonoids were among the subclasses with the highest number of annotated metabolites in both ionization modes (Figures 4c and 4d).

A total of 14 subclasses were categorized by the lipid analysis in ESI+ (Figure 4c) including ceramides; fatty amides; diradylglycerols; and triradylglycerols as the most significant: 25, 23, 13, 9, respectively. In the ESI− (Figure 4d), of a total of 13 subclasses, ceramides; neutral glycosphingolipids; bile acids; and fatty acids and conjugates were the major subclasses: 28, 10, 9 and 7, respectively. With exception of the ceramides subclass, the most abundant classes presented different classifications between ESI+ and ESI−. The same pattern is shown in the analysis of the polar compounds. This fact demonstrates the importance of the integrative analysis using both ESI modes for a comprehensive mapping of metabolites from fecal samples. The complete list of fecal metabolites putatively identified and its distribution can be found in SI section (Tables S4-S6), indicating the compounds classified into chemical families and the parameters supporting the identification.

The presence of a variety of endogenous compounds, such as bile acids, amino acids, fatty acids, vitamins, and carbohydrates in fecal samples has already been described by several authors[48,49] and are in agreement with our findings. Furthermore, according to Trošt *et al.*,[50] amino acids, fatty acids, carboxylic acids, benzene compounds and ceramides, triacylglycerides and diacylglycerides are classes of compounds found in human fecal samples. Choy *et al.*[51] have described hydroxylated phenolic acid metabolites in feces, while Schoeler *et al.*[52] have described lithocholic acid and deoxycholic acid as secondary bile acids produced by the gut microbiome via primary bile acids modification.

Molecular networking

A visual representation of the degree of chemical similarity among all MS/MS spectra datasets from HILIC-amide, RP-C$_{18}$ and CSH-C$_{18}$ were evaluated using molecular networking (MN) approach aiming to assess the chemical space of the metabolites.[53,54] The clusters from the ESI+ network is shown in Figure 5 (the complete networking is presented in Figure S1, SI section). Each node represents molecules that were colored according to the chromatographic column used (red: HILIC-amide, blue: RP-C$_{18}$, and green: CSH-C$_{18}$). Increasing the distance between the nodes correlates with the chemical dissimilarity between them (e.g., a and b *vs.* c, Figure 5). Compounds annotated through the input library were shaped like arrowheads, while circles indicate unknowns. This networking analysis can be used to extend the possibility of propagation of the structural annotation of unknown features connected to database matched features. However, the purpose of the MN analysis described here was to show the complexity of fecal samples in terms of metabolites and the importance of using complementary extractions and separation mechanisms rather than to deeply explore each detected feature in the full networks view.

The chemical features of each analytical strategy analyzed as ensembles determined the characteristic of the chemical space. Analyzing the chemical family's networks, not unexpectedly, it was shown that several nodes for common features from the different datasets present a high degree of similarity. This is noted by the different connections between the nodes and the number of edges involving a node and its immediate neighbors, such as for cholic acid (area 1, d, Figure 5). High network assortativity is an attribute given to the features with a high degree of similarity, emerging multiples correlations between the connected nodes.[54] These features can be seen in areas 1, 3 and 4, (Figure 5) and among the annotated bile acids, deoxycholic acid, 3-ketopetromyzonol and 12-ketodeoxycholic acid (e, f, and g, Figure 5) emerged from three different chromatographic columns. This finding
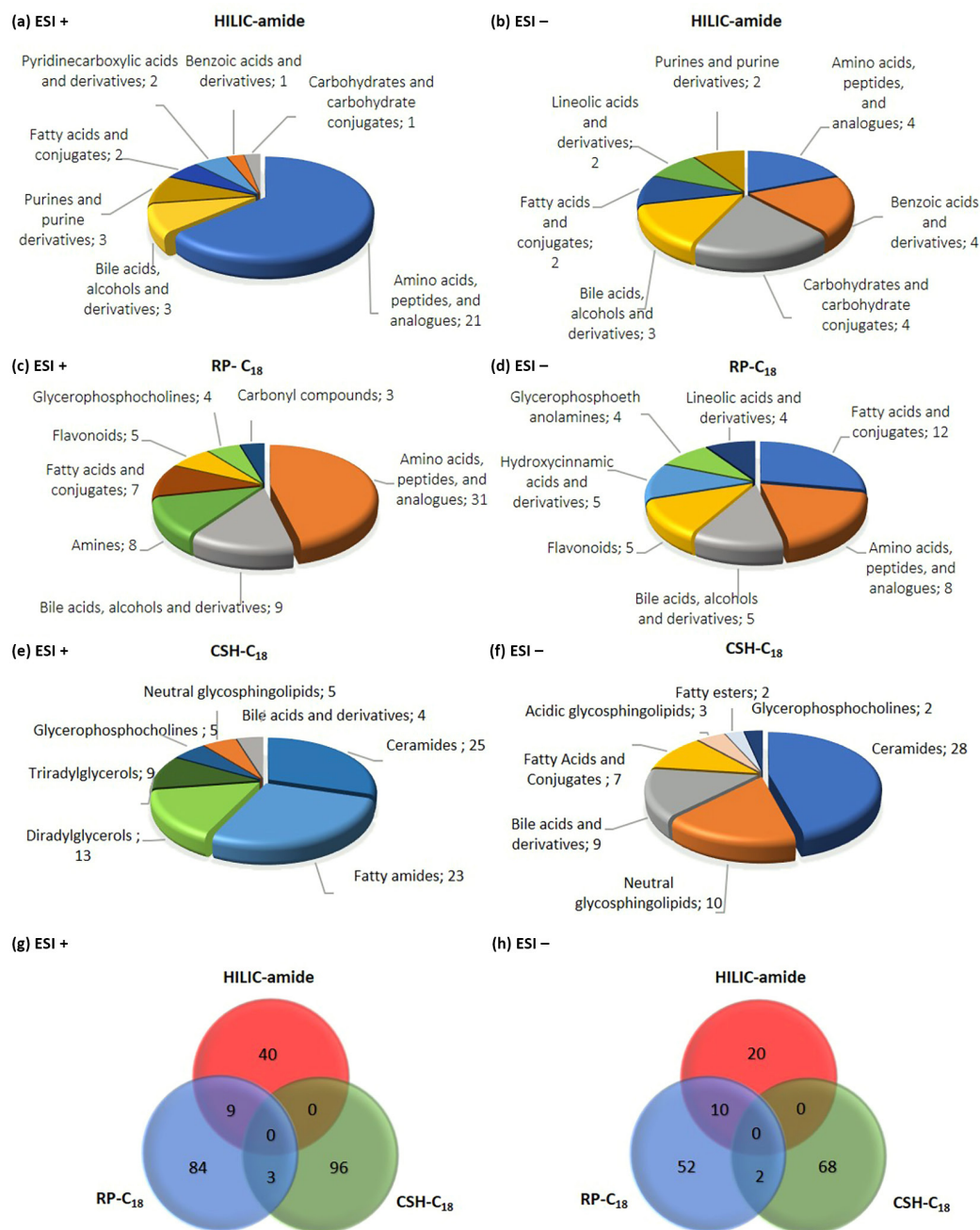
Figure 4. Chemical classification (a-f) and Venn diagram (g and h) of metabolites annotated in dog fecal samples by LC-HRMS/MS.

shows the relevance of the analytical integration strategies for better recognition of the chemical space. Other sterol lipids (ST) annotated exclusively by the data acquired from the CSH-C_{18} column can be observed in area 4 of Figure 5. The multiple correlations and high network assortativity between the ST metabolite nodes (24:1; O4/16:0), ST (24:1; O4/18:1) and ST (24:1; O4/24:1) demonstrate the high degree of similarity between these compounds. Nevertheless, it is possible to observe in areas 2 and 5 of Figure 5 that many features were not connected across the different datasets, as a hub with low assortativity. This

also highlights the importance of such a pipeline proposed here to cover a broad range of metabolites with distinct chemical properties.

Combined methods to enhance the metabolome coverage

To further understand how the proposed pipeline expanded the metabolites coverage connecting the three chromatographic methods (HILIC-amide, RP-C_{18} and CSH-C_{18}) and different ESI polarities compared to a single chromatographic method, it was performed a
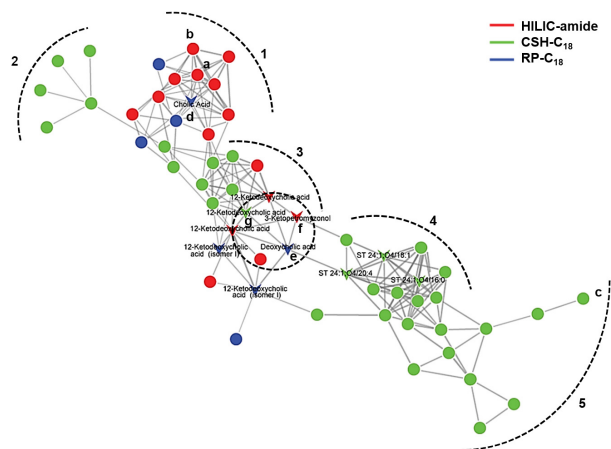
Figure 5. Representative chemical space network from the LC-HRMS/MS molecular networking analysis using a HILIC-amide, RP-C$_{18}$ and CSH-C$_{18}$ columns. Nodes were colored according to the chromatographic columns and shaped as arrowheads for annotated and circles for unknown compounds. The letters a to g represents the comparison of the numbers of connections between the nodes. The numbers 1 to 5 represent areas with different degrees of similarity between the nodes.

hybrid analysis using a Venn diagram (Figures 4g and 4h). A total of 360 unique metabolites were annotated by LC-HRMS/MS, 220 for ESI+ and 140 for ESI− analyses. High complementarity was found in the combination of the three methods and polarity modes. The HILIC method provided 60 unique polar metabolites and the RP-C$_{18}$ and CSH-C$_{18}$ methods contributed with 136 and 164 metabolites, respectively, adding compounds of medium polarity and lipids to the chemical space. Only 24 metabolites were in common from one or two of the methods, corresponding mostly to classes of amino acids, peptides, and bile acids, which presented amphipathic properties.

A large number of metabolites were preferentially ionized in the ESI+, such as compounds from the classes of carbonyl compounds, fatty acid esters, and glycosyldiradylglycerols. Compounds classes, such as sugar acids, pyrimidine nucleosides, and phosphosphingolipids preferentially ionized in ESI−. Additionally, 32 compounds, that is, 8.5% of the total annotated metabolites were detected in both polarities, such as cholic acid (RP-C$_{18}$), hypoxanthine (HILIC-amide) and ceramide (Cer) 18:0;3O/20:0;(2OH) (CSH-C$_{18}$). Overall, this strategy of combining methods demonstrated an impressive increase in metabolites assignment, underlining the importance to develop a pipeline analyzing the samples using both ionization polarities and different chromatographic separations to guarantee the expansion of metabolites coverage in an untargeted methodology.

Some approaches can be used to translate the assigned metabolites into a biochemically relevant context using pathway analysis. This facilitates metabolite data visualization and interpretation through the knowledge of

the metabolic pathways via biochemical differences within investigated conditions (e.g., control *vs.* disease).[55] The application of these approaches in the context of this project aims to comprehend the scope of the multiple analytical conditions and total annotated metabolites within common biochemical pathways.

Metabolites from six annotated datasets (HILIC-amide, RP-C$_{18}$ and CSH-C$_{18}$ in both ESI+ and ESI−) were subjected to pathway analysis using MetaboAnalyst 4.0[36] and the results are shown in Figure 6 and Table 1. Considering the pathway impact score, calculated based on the number of matched metabolites from datasets to a particular metabolic pathway (threshold > 0.1), the top pathways ($p < 0.05$) were seen as linoleic acid metabolism; sphingolipid metabolism; histidine metabolism; phenylalanine, tyrosine and tryptophan biosynthesis and phenylalanine metabolism. The metabolites identified in each pathway are highlighted in Figure 6.
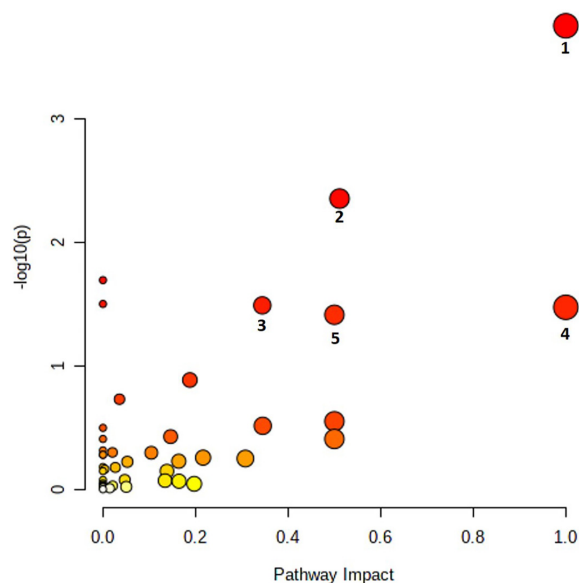

Figure 6. Differentially regulated metabolic pathway analysis from the annotated metabolites of the LC-HRMS analysis in both ESI+ and ESI− using a HILIC-amide, RP-C$_{18}$ and CSH-C$_{18}$ columns.

Several metabolite disorders can be related to metabolic diseases.[56,57] Deregulation in the linoleic acid metabolism, the pathway with the greatest impact value (1), have been reported from various inborn errors of metabolism.[58,59] This metabolic pathway act as precursors for the endogenous synthesis of longer-chain fatty acids such as eicosapentaenoic acid and docosahexaenoic acid after the metabolization of food-derived linoleic acid by the gut microorganism.[59] This process is essential for the maintenance of immune functions, brain activity and visual stimuli.[60]

Key metabolites from linoleic acid metabolism from different chromatographic columns and ESI modes were

Table 1. Correlation between the significant pathway analysis results with the matched metabolites

Identification	Pathway	Matched metabolites	Impact
1	linoleic acid metabolism	linoleate; phosphatidylcholine; 9(10)-EpOME; 12(13)-EpOME	1
2	sphingolipid metabolism	sphinganine; sphingomyelin; sphingosine; *N*-acylsphingosine; glucosylceramide; phytosphingosine	0.51
3	histidine metabolism	L-glutamate, urocanate; L-histidine; *N*(pros)-methyl-L-histidine	0.34
4	phenylalanine, tyrosine and tryptophan biosynthesis	L-phenylalanine; L-tyrosine	1
5	phenylalanine metabolism	phenylacetaldehyde; L-phenylalanine; L-tyrosine	0.5

9(10)-EpOME: 9,10-epoxyoctadecenoic acid.

annotated: linoleic acid from RP-C_{18} (ESI+ and ESI–), phosphatidylcholine (16:0/16:0) from CSH-C18 (ESI+) analyses, 9(10)-EpOME (9,10-epoxyoctadecenoic acid) from HILIC-amide (ESI+), and 12(13)-EpOME from RP-C_{18} (ESI+). Evaluation on changes in these metabolites are often correlated with the production of fatty acids and the maintenance of homeostasis.[61]

These observations can be considered as a proof-of-concept of a successful application of combined analytical strategies, described here as a pipeline for fecal metabolome coverage by LC-HRMS, to comprehensively annotate the metabolome of fecal samples in untargeted metabolomics within the context of systems biology studies of metabolism.

Conclusions

We have established a pipeline for a comprehensive analysis of the fecal metabolome using LC-HRMS/MS. For this, a combined strategy using a monophasic and a biphasic extraction and the chromatographic separation of compounds in columns with different selectivity (HILIC-amide, CSH-C_{18} and RP-C_{18}) were applied, allowing the analysis of high polar to weakly and nonpolar metabolites by LC-HRMS. This approach resulted in the annotation of 376 compounds from 70 different chemical classes.

The molecular networking analysis highlighted the complexity of the fecal sample chemical space and the chemical similarity of annotated compounds from the different LC-HRMS analyses. Whereas the results from the pathway analysis demonstrated the importance of a high number of annotated compounds to increase the pathway impact score.

This proof-of-concept study using a pool of dog feces can be used to expand our understanding of the fecal metabolome, its role in the host-gut microbiome relationship, and the impact of the environment, diet, and disease in this metabolome. This can ultimately lead to better diagnostic assays using the fecal matter.

Supplementary Information

The supplementary information (parameters used for processing the MS data using the MS-Dial software, the complete molecular network constructed with datasets from HILIC-amide, RP-C_{18} and CSH-C_{18}) are available free of charge at http://jbcs.sbq.org.br as PDF file.

The complete list of fecal metabolites putatively identified and its distribution in subclasses are available free of charge at http://jbcs.sbq.org.br as PDF file.

Acknowledgments

Author Contributions

Marina A. Alves were responsible for conceptualization, formal analysis, investigation, methodology, project administration, supervision, visualization, writing original draft, writing-review and editing; Ana Carolina R. da Silva for formal analysis, investigation, visualization, writing-review and editing; Clarisse L. Torres for formal analysis, investigation, visualization, writing-review and editing; Lana R. de Almeida for data curation, investigation, resources, writing-review and editing; Ana Maria O. Mastella for data curation, investigation, resources, writing-review and editing; Ricardo M. Borges for investigation, writing-review and editing; Rafael Garrett for conceptualization, formal analysis, funding acquisition, investigation, methodology, project administration, resources, supervision, visualization, writing-review and editing.

References

1. Cheng, K.; Brunius, C.; Fristedt, R.; Landberg, R.; *Metabolomics* **2020**, *1*, 46.

2. Xu, J.; Zhang, Q. F.; Zheng, J.; Yuan, B. F.; Feng, Y. Q.; *TrAC, Trends Anal. Chem.* **2019**, *112*, 161.

3. Yap, T. W. C.; Leow, A. H. R.; Azmi, A. N.; Callahan, D. L.; Perez-Perez, G. I.; Loke, M. F.; Goh, K. L.; Vadivelu, J.; *Front. Microbiol.* **2017**, *8*, 536.

4. Pedersen, H. K. V. G.; Nielsen, H. B.; Hyotylainen, T.; Nielsen, T.; *Nature* **2016**, *535*, 376.

5. Zhou, H.; Sun, L.; Zhang, S.; Zhao, X.; Gang, X.; Wang, G.; *Front. Endocrinol.* **2020**, *11*, 125.

6. Witkowski, M.; Weeks, T. L.; Hazen, S. L.; *Circ. Res.* **2020**, *127*, 553.

7. Slingerland, A. E.; Schwabkey, Z.; Wiesnoski, D. H.; Jenq, R. R.; *Front. Immunol.* **2017**, *8*, 400.

8. Aleman, F. D. D.; Valenzano, D. R.; *PLoS Pathog.* **2019**, *15*, e1007727.

9. Carlos, G.; dos Santos, F. P.; Fröehlich, P. E.; *Metabolomics* **2020**, *16*, 16.

10. Read, M. N.; Holmes, A. J.; *Front. Immunol.* **2017**, *8*, 538.

11. Hitchings, R.; Kelly, L.; *Trends Pharmacol. Sci.* **2019**, *40*, 495.

12. Sarma, S. J.; Lei, Z.; Rosenfeld, C. S.; Ericsson, A.; Sumner, L. W.; *Bioanalysis* **2020**, *12*, 351.

13. Karu, N.; Deng, L.; Slae, M.; Guo, A. C.; Sajed, T.; Huynh, H.; Wine, E.; Wishart, D. S.; *Anal. Chim. Acta* **2018**, *1030*, 1.

14. Aldana, J.; Romero-otero, A.; Cala, M. P.; *Metabolites* **2020**, *10*, 231.

15. Johnson, E. L.; Heaver, S. L.; Waters, J. L.; Kim, B. I.; Bretin, A.; Goodman, A. L.; Gewirtz, A. T.; Worgall, T. S.; Ley, R. E.; *Nat. Commun.* **2020**, *11*, 1.

16. Zeng, Y.; Lin, Y.; Li, L.; Li, Y.; Zhang, X.; Wang, M.; Chen, Y.; Luo, L.; Lu, B.; Xie, Z.; Liao, Q.; *J. Chromatogr. B: Anal. Technol. Biomed. Life Sci.* **2019**, *1110-1111*, 133.

17. Cesbron, N.; Royer, A. L.; Guitton, Y.; Sydor, A.; le Bizec, B.; Dervilly-Pinel, G.; *Metabolomics* **2017**, *13*, 99.

18. López-Bascón, M. A.; Calderón-Santiago, M.; Argüello, H.; Morera, L.; Garrido, J. J.; Priego-Capote, F.; *Talanta* **2019**, *199*, 303.

19. Yu, M.; Jia, H.; Zhou, C.; Yang, Y.; Zhao, Y.; Yang, M.; Zou, Z.; *J. Pharm. Biomed. Anal.* **2017**, *138*, 231.

20. Respondek, F.; Gerard, P.; Bossis, M.; Boschat, L.; Bruneau, A.; Rabot, S.; Wagner, A.; Martin, J.-C.; *PLoS One* **2013**, *8*, e71026.

21. Zhou, Y.; Men, L.; Pi, Z.; Wei, M.; Song, F.; Zhao, C.; Liu, Z.; *J. Agric. Food Chem.* **2018**, *66*, 1591.

22. Quifer-Rada, P.; Choy, Y. Y.; Calvert, C. C.; Waterhouse, A. L.; Lamuela-Raventos, R. M.; *Mol. Nutr. Food Res.* **2016**, *60*, 2219.

23. Cheng, K.; Brunius, C.; Fristedt, R.; Landberg, R.; *Metabolomics* **2020**, *16*, 46.

24. Lamichhane, S.; Sen, P.; Dickens, A. M.; Orešič, M.; Bertram, H. C.; *Methods* **2018**, *149*, 3.

25. Hinnant, R. T.; Kothmann, M. M.; *J. Range Manage.* **1988**, *41*, 168.

26. Matyash, V.; Liebisch, G.; Kurzchalia, T. V.; Shevchenko, A.; Schwudke, D.; *J. Lipid Res.* **2008**, *49*, 1137.

27. Zalloua, P.; Kadar, H.; Hariri, E.; Abi Farraj, L.; Brial, F.; Hedjazi, L.; le Lay, A.; Colleu, A.; Dubus, J.; Touboul, D.; Matsuda, F.; Lathrop, M.; Nicholson, J. K.; Dumas, M. E.; Gauguier, D.; *Lipids Health Dis.* **2019**, *18*, 38.

28. Silva, A. C. R.; da Silva, C. C.; Garrett, R.; Rezende, C. M.; *Food Res. Int.* **2020**, *137*, 109727.

29. Virgiliou, C.; Sampsonidis, I.; Gika, H. G.; Raikos, N.; Theodoridis, G. A.; *Electrophoresis* **2015**, *36*, 2215.

30. Liu, X.; Ser, Z.; Cluntun, A. A.; Mentch, S. J.; Locasale, J. W.; *J. Visualized Exp.* **2014**, *87*, e51358.

31. Peñaloza, E.; Holandino, C.; Scherr, C.; de Araujo, P. I. P.; Borges, R. M.; Urech, K.; Baumgartner, S.; Garrett, R.; *Molecules* **2020**, *25*, 4006.

32. Tsugawa, H.; Cajka, T.; Kind, T.; Ma, Y.; Higgins, B.; Ikeda, K.; Kanazawa, M.; Vandergheynst, J.; Fiehn, O.; Arita, M.; *Nat. Methods* **2015**, *12*, 523.

33. Feunang, Y. D.; Eisner, R.; Knox, C.; Chepelev, L.; Hastings, J.; Owen, G.; Fahy, E.; Steinbeck, C.; Subramanian, S.; Bolton, E.; Greiner, R.; Wishart, D. S.; *J. Cheminf.* **2016**, *8*, 61.

34. Wohlgemuth, G.; Haldiya, P. K.; Willighagen, E.; Kind, T.; Fiehn, O.; *Bioinformatics* **2010**, *26*, 2647.

35. http://bioinformatics.psb.ugent.be/webtools/Venn/, accessed in March 2021.

36. Chong, J.; Soufan, O.; Li, C.; Caraus, I.; Li, S.; Bourque, G.; Wishart, D. S.; Xia, J.; *Nucleic Acids Res.* **2018**, *46*, W486.

37. Wang, M.; Carver, J. J.; Phelan, V. V.; Sanchez, L. M.; Garg, N.; Peng, Y.; Duy Nguyen, D.; Watrous, J.; Kapono, C. A.; Luzzatto-Knaan, T.; Porto, C.; Bouslimani, A.; Melnik, A. V.; Meehan, M. J.; Liu, W.-T.; Crüsemann, M.; Boudreau, P. D.; Esquenazi, E.; Sandoval-Calderón, M.; Kersten, R. D.; Pace, L. A.; Quinn, R. A.; Duncan, K. R.; Hsu, C.-C.; Floros, D. J.; Gavilan, R. G.; Kleigrewe, K.; Northen, T.; Dutton, R. J.; Parrot, D.; Carlson, E. E.; Aigle, B.; Michelsen, C. F.; Jelsbak, L.; Sohlenkamp, C.; Pevzner, P.; Edlund, A.; McLean, J.; Piel, J.; Murphy, B. T.; Gerwick, L.; Liaw, C.-C.; Yang, Y.-L.; Humpf, H.-U.; Maansson, M.; Keyzers, R. A.; Sims, A. C.; Johnson, A. R.; Sidebottom, A. M.; Sedio, B. E.; Klitgaard, A.; Larson, C. B.; Boya P, C. A.; Torres-Mendoza, D.; Gonzalez, D. J.; Silva, D. B.; Marques, L. M.; Demarque, D. P.; Pociute, E.; O, E. C.; Briand, E.; N Helfrich, E. J.; Granatosky, E. A.; Glukhov, E.; Ryffel, F.; Houson, H.; Mohimani, H.; Kharbush, J. J.; Zeng, Y.; Vorholt, J. A.; Kurita, K. L.; Charusanti, P.; McPhail, K. L.; Fog Nielsen, K.; Vuong, L.; Elfeki, M.; Traxler, M. F.; Engene, N.; Koyama, N.; Vining, O. B.; Baric, R.; Silva, R. R.; Mascuch, S. J.; Tomasi, S.; Jenkins, S.; Macherla, V.; Hoffman,

T.; Agarwal, V.; Williams, P. G.; Dai, J.; Neupane, R.; Gurr, J.; C Rodríguez, A. M.; Lamsa, A.; Zhang, C.; Dorrestein, K.; Duggan, B. M.; Almaliti, J.; Allard, P.-M.; Phapale, P.; Nothias, L.-F.; Alexandrov, T.; Litaudon, M.; Wolfender, J.-L.; Kyle, J. E.; Metz, T. O.; Peryea, T.; Nguyen, D.-T.; VanLeer, D.; Shinn, P.; Jadhav, A.; Müller, R.; Waters, K. M.; Shi, W.; Liu, X.; Zhang, L.; Knight, R.; Jensen, P. R.; Ø Palsson, B.; Pogliano, K.; Linington, R. G.; Gutiérrez, M.; Lopes, N. P.; Gerwick, W. H.; Moore, B. S.; Dorrestein, P. C.; Bandeira, N.; *Nat. Biotechnol.* **2016**, *34*, 828.

38. Nothias, L. F.; Nothias-Esposito, M.; da Silva, R.; Wang, M.; Protsyuk, I.; Zhang, Z.; Sarvepalli, A.; Leyssen, P.; Touboul, D.; Costa, J.; Paolini, J.; Alexandrov, T.; Litaudon, M.; Dorrestein, P. C.; *J. Nat. Prod.* **2018**, *81*, 758.

39. Nothias, L. F.; Petras, D.; Schmid, R.; Dührkop, K.; Rainer, J.; Sarvepalli, A.; Protsyuk, I.; Ernst, M.; Tsugawa, H.; Fleischauer, M.; Aicheler, F.; Aksenov, A. A.; Alka, O.; Allard, P. M.; Barsch, A.; Cachet, X.; Caraballo-Rodriguez, A. M.; da Silva, R. R.; Dang, T.; Garg, N.; Gauglitz, J. M.; Gurevich, A.; Isaac, G.; Jarmusch, A. K.; Kameník, Z.; Kang, K. B.; Kessler, N.; Koester, I.; Korf, A.; le Gouellec, A.; Ludwig, M.; Martin, H, C.; McCall, L. I.; McSayles, J.; Meyer, S. W.; Mohimani, H.; Morsy, M.; Moyne, O.; Neumann, S.; Neuweger, H.; Nguyen, N. H.; Nothias-Esposito, M.; Paolini, J.; Phelan, V. V.; Pluskal, T.; Quinn, R. A.; Rogers, S.; Shrestha, B.; Tripathi, A.; van der Hooft, J. J. J.; Vargas, F.; Weldon, K. C.; Witting, M.; Yang, H.; Zhang, Z.; Zubeil, F.; Kohlbacher, O.; Böcker, S.; Alexandrov, T.; Bandeira, N.; Wang, M.; Dorrestein, P. C.; *Nat. Methods* **2020**, *17*, 905.

40. Olivon, F.; Grelier, G.; Roussi, F.; Litaudon, M.; Touboul, D.; *Anal. Chem.* **2017**, *89*, 7836.

41. Rogers, S.; Ong, C. W.; Wandy, J.; Ernst, M.; Ridder, L.; van der Hooft, J. J. J.; *Faraday Discuss.* **2019**, *218*, 284.

42. Ernst, M.; Kang, K. B.; Caraballo-Rodríguez, A. M.; Nothias, L. F.; Wandy, J.; Chen, C.; Wang, M.; Rogers, S.; Medema, M. H.; Dorrestein, P. C.; van der Hooft, J. J. J.; *Metabolites* **2019**, *9*, 144.

43. Shannon, P.; Markiel, A.; Ozier, O.; Baliga, N. S.; Wang, J. T.; Ramage, D.; Amin, N.; Schwikowski, B.; Ideker, T.; *Genome Res.* **1971**, *13*, 426.

44. Sumner, L. W.; Amberg, A.; Barrett, D.; Beale, M. H.; Beger, R.; Daykin, C. A.; Fan, T. W. M.; Fiehn, O.; Goodacre, R.; Griffin, J. L.; Hankemeier, T.; Hardy, N.; Harnly, J.; Higashi, R.; Kopka, J.; Lane, A. N.; Lindon, J. C.; Marriott, P.; Nicholls,

A. W.; Reily, M. D.; Thaden, J. J.; Viant, M. R.; *Metabolomics* **2007**, *3*, 211.

45. Schymanski, E. L.; Jeon, J.; Gulde, R.; Fenner, K.; Ruff, M.; Singer, H. P.; Hollender, J.; *Environ. Sci. Technol.* **2014**, *48*, 2097.

46. Villaret-Cazadamont, J.; Poupin, N.; Tournadre, A.; Batut, A.; Gales, L.; Zalko, D.; Cabaton, N. J.; Bellvert, F.; Bertrand-Michel, J.; *Metabolites* **2020**, *10*, 490.

47. Schwaiger, M.; Schoeny, H.; El Abiead, Y.; Hermann, G.; Rampler, E.; Koellensperger, G.; *Analyst* **2019**, *144*, 220.

48. Sillner, N.; Walker, A.; Harrieder, E. M.; Schmitt-Kopplin, P.; Witting, M.; *J. Chromatogr. B: Anal. Technol. Biomed. Life Sci.* **2019**, *1109*, 142.

49. Begou, O.; Deda, O.; Agapiou, A.; Taitzoglou, I.; Gika, H.; Theodoridis, G.; *J. Chromatogr. B: Anal. Technol. Biomed. Life Sci.* **2019**, *1114-1115*, 76.

50. Trošt, K.; Ahonen, L.; Suvitaival, T.; Christiansen, N.; Nielsen, T.; Thiele, M.; Jacobsen, S.; Krag, A.; Rossing, P.; Hansen, T.; Dragsted, L. O.; Legido-Quigley, C.; *Sci. Rep.* **2020**, *10*, 885.

51. Choy, Y. Y.; Quifer-Rada, P.; Holstege, D. M.; Frese, S. A.; Calvert, C. C.; Mills, D. A.; Lamuela-Raventos, R. M.; Waterhouse, A. L.; *Food Funct.* **2014**, *5*, 2298.

52. Schoeler, M.; Caesar, R.; *Rev. Endocr. Metab. Disord.* **2019**, *20*, 461.

53. Wang, M.; Carver, J. J.; Phelan, V. V; Sanchez, L. M.; Garg, N.; Peng, Y.; Nguyen, D. D.; *Nat. Biotechnol.* **2017**, *34*, 828.

54. Vogt, M.; Stumpfe, D.; Maggiora, G. M.; Bajorath, J.; *J. Comput.-Aided. Mol. Des.* **2016**, *30*, 191.

55. Ivanisevic, J.; Want, E. J.; *Metabolites* **2019**, *9*, 308.

56. Prietsch, V.; Lindner, M.; Zschocke, J.; Nyhan, W. L.; Hoffmann, G. F.; *J. Inherited Metab. Dis.* **2002**, *25*, 531.

57. Pascale, A.; Marchesi, N.; Marelli, C.; Coppola, A.; Luzi, L.; Govoni, S.; Giustina, A.; Gazzaruso, C.; *Endocrine* **2018**, *61*, 357.

58. Fekete, K.; Decsi, T.; *Nutrients* **2010**, *2*, 965.

59. Devillard, E.; McIntosh, F. M.; Duncan, S. H.; Wallace, R. J.; *J. Bacteriol.* **2007**, *189*, 2566.

60. Thangavelu, S.; *Indian J. Pract. Pediatr.* **2010**, *12*, 181.

61. Latour, M. A.; Devitt, A. A.; Meunier, R. A.; Stewart, J. J.; Watkins, B. A.; *Poult. Sci.* **2000**, *79*, 817.